Journal of Research in Pharmacy

Research Article

www.jrespharm.com

Evaluation of platelet-derived growth factor loaded polycaprolactone/collagen core-shell nanofibers as guided tissue membrane

Mazdak LIMOEE[1], Mahsa RASEKHIAN[2], Pouran MORADIPOUR[1,3], Zahra POURMANOUCHEHRI[2], Leila BEHBOOD[1,4*]

1 Nano Drug Delivery research center, Kermanshah University of Medical Sciences, Kermanshah, Iran.
2 Pharmaceutical sciences research center, School of Pharmacy, Kermanshah University of Medical Sciences, Kermanshah, Iran
3 School of Chemical Engineering, College of Engineering, University of Tehran, Tehran, Iran.
4 Pharmaceutical sciences research center, Health Institute, Kermanshah University of Medical Sciences, Kermanshah, Iran.

* Corresponding Author. E-mail: lbehbood22@gmail.com, (L.B.); Tel. +98-917-411 39 58.

Received: 25 December 2022 / Revised: 4 June 2024 / Accepted: 6 June 2024

ABSTRACT: Guided tissue regeneration (GTR) is a dental surgical procedure that uses barrier membranes to guide the growth of bone, tissue, or gingiva in small places for proper function, beauty, or restoration of the prosthesis. Recently, many efforts have been made to accelerate tissue repair by adding agents such as growth factors to the GTR structure in a targeted and controlled manner of drug release, which makes the treatment more effective and reduces its side effects. The aim of this study was the preparation and evaluation of growth factor-loaded, biodegradable fibers, as a GTR membrane in oral cavity disease. In this study, two electrostatic systems of polycaprolactone (PCL) (shell) and platelet-derived growth factor (PDGF) loaded collagen (core) were fabricated via coaxial electrospinning. Core-shell fibers were analyzed by FTIR, SEM, TEM, and ELISA techniques to determine the PDGF release and supplemented via *in-vitro* cytotoxicity, proliferation, and real-time PCR investigation. FT-IR shows that the fiber's constituents do not interfere with each other. The diameter of the nanofibers is in the range of 400 nm, and the results of the TEM images show that the core-shell structure is formed. PDGF is released from fibers in a controlled manner. The fibers do not show any cellular toxicity, have a positive effect on cell proliferation, and increase the number of cells.

KEYWORDS: Electrospinning; core-shell; collagen; polycaprolactone; platelet-derived growth factor; Guided Tissue Regeneration.

1. INTRODUCTION

Periodontal diseases represent a common health obstacle that can involve millions of people worldwide and lead to loss of connective tissue and bone or even tooth loss in its severe form "Periodontitis"[1]. Periodontal tissue surgery was the only known method for repairing damaged tissue. Recently, the Guided Tissue Regeneration (GTR) and Guided Bone Regeneration (GBR) methods have received a lot of attention. These methods use a blocking membrane attached to the epithelium or gums and alveolar bone to prevent its early attachment and from becoming defective tissue. The primary (progressive) cells left in the cartilage, adjacent to the alveolar bone or blood, can detect the root zone and differentiate into a support for the new periodontium, which is associated with the formation of new Periodontal Ligament (PDL) and cementum bones [2].

GTRs should meet the requirements including biocompatibility that allow the membrane to integrate with the host tissue without causing an inflammatory response, proper degradation profile to adapt to the formation of new tissue, appropriate mechanical and physical properties to be able to fit *in vivo* conditions, and high durability to prevent membrane collapse and maintain its function [3, 4]. Absorbable GTRs have been used to prevent second surgery to remove GTR from tissue. Most synthetic polymers used in absorbable membranes have an ester structure such as polyglycolic acid (PGA), polylactic acid (PLA),

How to cite this article: Limoee M, Rasekhian M, Moradipour P, Pourmanouchehri Z, Behbood L. Evaluation of platelet-derived growth factor loaded Polycaprolactone/Collagen core-shell nanofibers as Guided Tissue Membrane. J Res Pharm. 2025; 29(2): 820-832.

ISSN: 2630-6344

https://doi.org/10.12991/jrespharm.1666362

polycaprolactone (PCL), and their copolymers. Polymers of natural origin, such as tissue-derived collagens, are also used in the structure of these membranes [4, 5]. Collagens as the most abundant protein and the main component of the ECM of animal tissue have brilliant advantages such as non-cytotoxicity, good proliferation, cell adhesion, biocompatibility, biodegradability, absorbability, and low antigenicity [6-8]. The use of Col in guided bone/tissue regeneration is still challenging because of its rapid degradation rate and insufficient tensile strength. Therefore, it seems PCL as proper polymer could contribute to the improvement of barrier membranes.

Normal tissue regeneration is the ultimate goal for tissue that has suffered trauma, surgery, or infectious disease. Growth factors are proteins that act locally or systemically so that they can affect cell growth and function in several ways. The growth factor functions to regenerate damaged tissue through biomimetic processes or to mimic the methods used during embryonic and postnatal development for the growth and development of the body [9, 10]. Within the last decade, cellular and molecular biology provided the context for discovering the role of growth factors and their participation in various stages of wound healing [11, 12]. PDGF was the first growth factor to be studied in pre-clinical studies and peripheral reconstruction. In the culture medium containing periodontal cells such as gums, PDL fibroblasts, cementoblasts, peri-osteoblasts, and osteoblasts that were exposed to PDGF, cell proliferation, migration, and matrix synthesis were observed. PDGF-BB is the most effective in the proliferation of PDL fibroblasts and matrix biosynthesis [13].

In the last two decades, researchers have paid special attention to nanofibers. Its features include a high surface-to-volume ratio, flexibility in surface modification, good mechanical properties, low base weight, high porosity, favorable economic efficiency, complete coherence, and a micro-scale pore network [14]. These structures have a wide variety of applications that are successfully used in medicine and drug delivery including wound dressing, scaffolding for tissue engineering, implants, and drug delivery systems [15]. Coaxial (two-fluid) electrospinning is one of the most successful modifications that increase the quality and performance of the final nanofiber structure. In this method, two different fluids are transferred independently through two different pumps and a coaxial nozzle [16, 17]. The outer fluid, like a shell, encapsulates the inner fluid [18]. Among the most important applications of core-shell nanofibers are the following: Placing an unstable compound as a shell to isolate it and minimize changes in the decomposition of the compound due to the active and reactive environment. Release of core material after a certain period to be transferred to its special receiver. Increase the mechanical strength of the fiber used by the core. Adding biocompatible shells reduces the toxicity of the core material (commonly used in tissue engineering). All influential parameters in conventional electrospinning are also effective in coaxial electrospinning. In addition, parameters related to shell and core solutions are added (viscosity, surface tension, electrical conductivity, etc.) [19-21].

Similar research has shown that the release of growth factors in less than 10 days may delay the healing of the lesion. So, our aim in this study was to investigate and introduce PCL/Col fiber mats with different amounts of PDGF fabricated by the coaxial electrospinning method to prolong the release of growth factors from nanofibers (Figure 1). Properties of fabricated nanofibers such as surface morphology and chemical properties were fully investigated. We also evaluate nanofibers ability to accelerate cell proliferation and osteogenic-related gene expression.

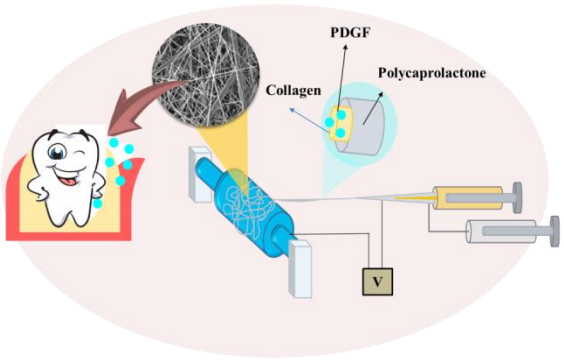

Figure 1. The design and preparation of the PCL/Col core-shell membranes loaded with PDGF for guided tissue regeneration.

2. RESULTS AND DISCUSSION

Periodontal diseases are one of the prevalent diseases, impacting approximately 30-40% of the population [22]. GTR and GBR membranes are used to treat this disease by placing them in the dental cavity. There has been extensive research on these membranes, which have shown good profile such as strength, biocompatibility, and biodegradability [23-25]. Additionally, they have the capability to act as a drug delivery system by loading drugs [2]. Studies have also shown that using growth factors loaded in mats can accelerate the healing process of the lesion [26]. Among the various barrier used to produce these membranes, nanofibers have been found to be the efficient and straightforward due to their good release profile and the uniformity of the fiber diameter [4].

2.1. Optimizing electrospinning parameter

Collagen electrospinning was challenging thanks to the stability of collagen tertiary structure and also the lack of necessary viscoelastic response limited jet stabilization [27]. Hence, developing methods based on using polymer support can be useful. Our previous study has shown that PCL/Col core-shell structure fibers could provide suitable mechanical properties with proper structure and morphologies. After modifying the electrospinning parameter, the optimum conditions were set at 16 kV, 0.25 ml/h, and the flow ratio of the core to the shell was 1 to 3 [28].

2.2. Characterization of nanofibers

The morphological properties of the prepared PCL/Col and PDGF@PCL/Col fibers were analyzed using SEM and TEM. Results for SEM images of the PCL/Col fibers are shown in Figure 2A, which revealed non-uniform fiber morphologies. The swelling of the shell surface indicates the low solvent boiling point of the shell (a mixture of dichloromethane and ethanol) led to its rapid evaporation during electrospinning and the creation of holes on the fiber surface. This porosity increases the surface-volume ratio, which results in better drug delivery and better adhesion to the damaged tissue surface [29]. By TEM imaging (Figure 2B), the core-shell structure of nanofiber can be seen, where the core is the Col with a diameter of 203 nm and the light grey fiber surrounding the core is the PCL with a diameter of 388 nm. According to Figure 2C, SEM was used to evaluate fibers' biodegradation after placing them in an aqueous medium. The distribution histogram (Figure 2D) shows that the diameter of fibers (5445 ± 3449 nm [28]) decreased after the treatment with the buffer to 814 ± 556 nm. Considering the decrease in the average size after soaking in the buffer, it can be concluded that the fibers with large diameters were related to collagen fibers that were dissolved in an aqueous medium. In general, smaller diameter nanofibers remained better in the aqueous medium and were probably related to the core-shell structure.

An SEM image of PDGF@PCL/Col is displayed in Figure 2E. Most fibers have the same diameter and good uniformity. The shape of a rosary bead is quite clear and shows the swelling of the core and the trapping of growth factors in that area. The growth factor of PDGF, with a molecular weight of 24 kDa and a relatively large size, appears to cause the nanofiber structure to swell in that area. The mean diameter of PCL/Col reached 4991± 2737 nm after the GF was loaded. This increase compared to PCL/Col nanofibers related to the PDGF with high molecular weight which was loaded and the observed decrease compared to Col fibers due to the increase in charge caused by GF and thus increased the conductivity of the polymer solution.

The influence of the PDGF on the nanofiber chemical structure was also investigated by FT-IR. The FTIR spectra of the PCL/Col before [28] and after electrospinning by PDGF were illustrated in Figure 3. As discussed in the previous study, the characteristic infrared bands of PCL/Col were observed at 3383 cm^{-1} (hydroxyl stretching vibration of Col), 2947 cm^{-1}, and 2873 cm^{-1} (CH_2 stretching vibration of PCL), 1728 cm^{-1} (C=O stretching vibration of PCL), 1647 cm^{-1} and 1546 cm^{-1} (amine groups of proteins in Col), and 1168 cm^{-1} (asymmetric C-O-C stretching vibration of PCL) (28). The FTIR spectrum of PDGF@PCL/Col mats shows a similar structure to PCL/Col fibers with different intensities. The characteristic peaks of PCL/Col were exhibited no significant shifts ruling out the possibility of covalently bonded between PDGF and Col. Furthermore, due to the protein structure of Col and PDGF, the PDGF peak was masked by Col. But the slight shifting of 1647 cm^{-1} peaks toward the lower wavenumber indicates the formation of hydrogen interaction between Col and PDGF.

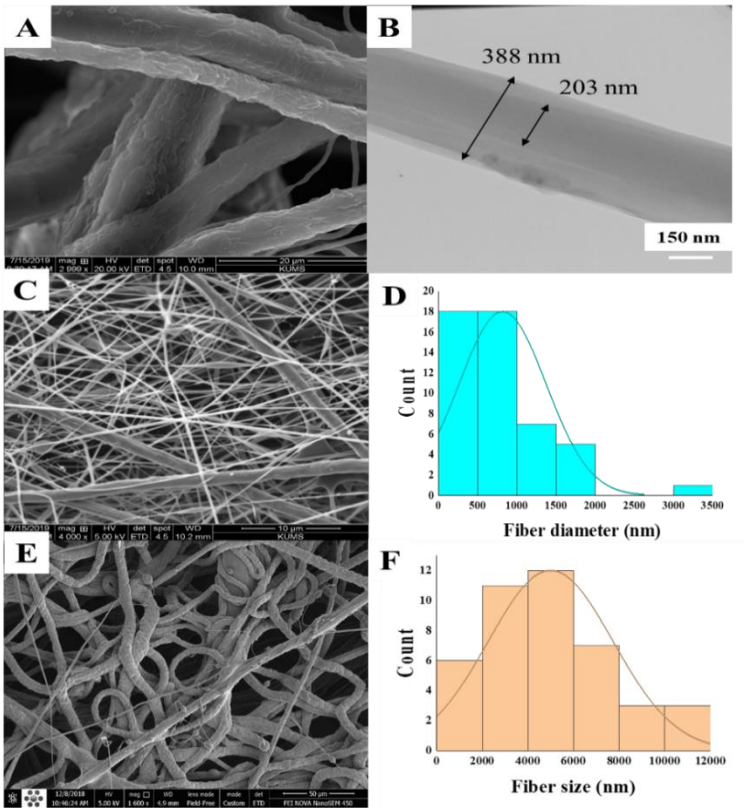

Figure 2. Morphology of PCL/Col nanofibers; (A) SEM image with a magnification of 20 µm, (B) TEM image with a magnification of 150 nm, (C) SEM image, and (D) Size distribution of PCL/Col nanofibers after immersion in phosphate buffer (pH 7.4) for 24 h, (E) FE-SEM images of PDGF@PCL/Col nanofibers, and (F) diameter distributions of the PDGF@PCL/Col nanofibers.

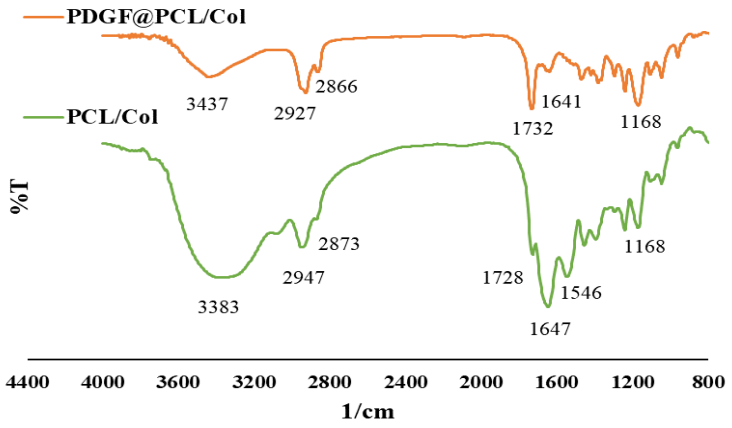

Figure 3. FT-IR spectra of the PCL/Col (28) and PDGF@PCL/Col nanofibers.

2.3. *In-vitro* Release profile

Growth factor release from optimal fibers was evaluated at three different concentrations of 0.312, 0.625, and 1.25 ng/mg of growth factor in a polymer solution. Figure 4 shows the rate of growth factor release over 40 days. The prepared nanofibers exhibited good sustained-release properties *in vitro*. The average cumulative release from the nanofibers was 99% at the end of the period and sustained release was demonstrated for 40 days. The release behavior of 0.625 and 1.25 fibers are similar while the PDGF release

from 0.325 fibers was slower than others in a way that the release rate was still zero after three weeks. The concentration of 0.312ng/mg has a delayed-release model due to the low concentration of growth factor and has a very low release in the first few days. At a concentration of 0.625ng/mg, the release was controlled and at a concentration of 1.25ng/mg, due to the higher amount of growth factor, a burst release occurred first and then it became a controlled release. Considering that the structure of the final fiber was in the form of a core-shell, the initial burst release in the nanofibers with 0.625 and 1.25 ng of PDGF was related to the areas where the collagen fiber did not have a PCL coating and led to the rapid dissolution of collagen and fast release of PDGF, especially in fibers with a higher PDGF content.

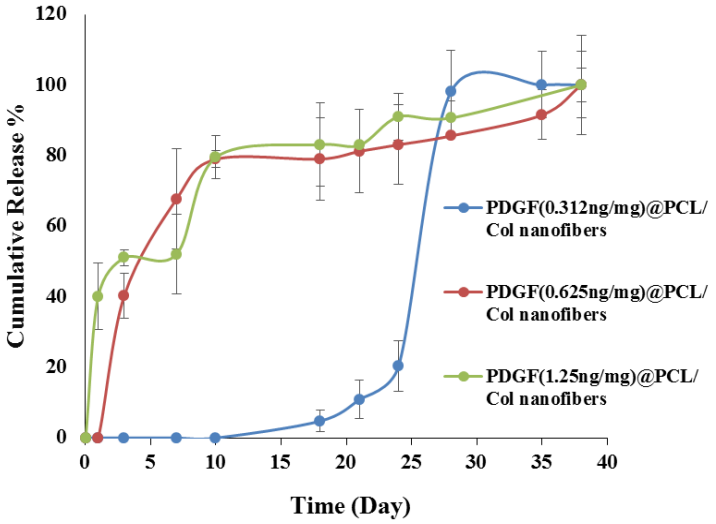

Figure 4. The release profile of various concentrations of PDGF in PCL/Col nanofibers.

Different models of release kinetics including zero-order, first-order, and Higuchi models were used and drug release in each concentration was reported with the mentioned models. Table 1 shows the linear and regression equations of the nanofibers release models. The first-order model is the main release model for fibers with a concentration of 0.312 ng/mg of PDGF. The regression of different models is not very close to each other and has a large distance from the ideal regression, which is one. It seems to be due to the low concentration obtained from the sample. The test error is likely to be high, so this release model is not very reliable. Furthermore, it was concluded that the Higuchi model was more suitable than other models for PDGF (0.625ng/mg) and (1.20 ng/mg) @ PCL/Col fibers. However, the regression of the Higuchi model is very low compared to the ideal regression.

Owing to the GF release from fibers in all three concentrations, PDGF (0.625ng/mg) @ PCL/Col fiber was considered as an optimal concentration. This release followed the Higuchi model and lasted for 40 days. The positive point of this study is that on the twentieth day, drug release reaches ~85%, while previous studies have shown that 90% release of GF from fiber occurred during the first 24 to 48 hours [30, 31]. Considering that the patient takes anti-inflammatory drugs such as non-steroidal anti-inflammatory drugs after surgery and these drugs reduce cell migration while GF increases cell migration, the interaction of these two drugs must be considered. They were in conflict and had pharmacological interactions with each other. The release findings can be promising to reduce this interference due to the sudden decrease in drug release in the first week of release [32, 33].

Table 1. Linear equation and regression of 0.625ng/mg PDGF fibers in 3 main models.

Release Model	Zero Order	First Order	Higuchi
PDGF(0.312ng/mg)@PCL/Col nanofibers	y= 4.1061x-99.632 R^2=0.6565	y= 2.4802x-13.494 R^2=0.6855	y= 26.15x-125.27 R^2=0.5896
PDGF(0.625ng/mg)@PCL/Col nanofibers	y= 1.8454x+26.938 R^2=0.6157	y= 1.1315x+65.429 R^2=0.2836	y= 13.562x+8.8609 R^2=0.7363
PDGF(1.25ng/mg)@PCL/Col nanofibers	y= 2.0686x+35.988 R^2=0.7359	y= 1.2193x+67.769 R^2=0.2623	y= 14.822x+16.744 R^2=0.8944

2.4. MTT assay

Since these nanofibers will be planted inside the tissue, they must have no toxic or harmful effects on human tissue. For this purpose, the cytotoxicity of prepared nanofibers that were not loaded with GF was examined on MG-63 cells (Figure 5). Given that the two polymers of Col and PCL in the manufacture of GTR were approved by the US Food and Drug Administration (FDA), we expected that PCL/Col fibers would have no toxic effects. As shown in Figure 5, during the 24 h of culturing with PCL/Col nanofibers, the cells grew compared to the control, which verified the nanofiber membrane was not toxic to MG-63 cells and had good biocompatibility. Many studies have investigated the effect of Col on cell proliferation. This effect can be due to cell induction by Col through integrin-mediated [34]. In confirmation of the present findings, Khatami *et al* showed that the addition of Col to alginate-nano-silica microspheres leads to increased cell proliferation and the expression of osteocalcin and BMP-2 in MG-63 cells [35]. Furthermore, it was revealed that collagen hydrolysates enhance cell proliferation in MG-63 cells up to 130% compared to the control group [36].

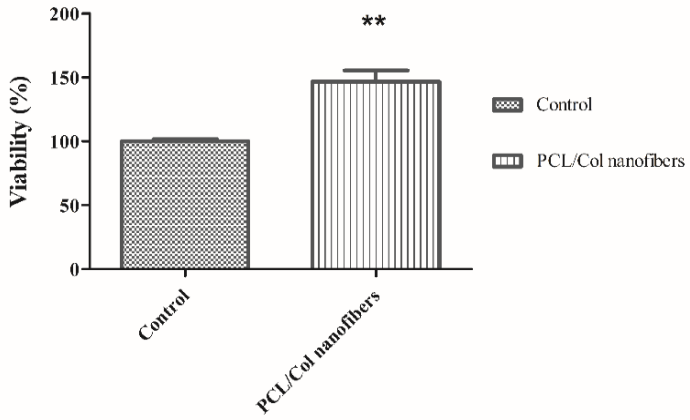

Figure 5. Cell viability of MG-63 cells after culturing with PCL/Col nanofibers for 24 h using MTT assay. Data are represented as mean ± SD from three independent tests. (**P < 0.01 vs. control).

2.5. Cell proliferation

The proliferation of damaged tissue cells must be increased to accelerate lesion healing. *In vitro* cell proliferation of prepared core-shell nanofibers was assessed for 40 days. As shown in Figure 6, the results of cell proliferation showed that the fibers containing PDGF in all three concentrations increased the proliferation of MG-63 cells. The best proliferation rate was for nanofibers with 0.625 ng of PDGF compared to other ones. PDGF cumulative release from 0.312 ng/mg PDGF fibers before day 21 is insignificant and the induction of cell proliferation changes accordingly. The result of cell proliferation for 0.625 ng/mg PDGF and 1.25 ng/mg PDGF fibers is in complete agreement with the results that were obtained from the release test. The release chart initially shows a sudden release of growth factor which corresponds to an increase in cell proliferation in the early days. A decrease in cell proliferation values in all groups after day 30 could related to the completion of GF release in the last week which did not sufficiently stimulate cell proliferation [37]. This excellent result indicates that the growth factor activity was not affected by the electrospinning process and when supplied to the cells, stimulates cell division. Studies have shown that the PDGF has no cytotoxicity effects either alone or by collagen carriers, which is consistent with the findings of this study [31, 38, 39].

According to the results, nanofiber 0.312 ng/mg had a delayed release due to the low concentration of the growth factor. Nanofiber 0.625 ng/mg had a controlled release and had the best cell proliferation results. Nanofiber 1.25 ng/mg had a sudden release due to the high concentration of growth factor, which confirms the results of release and cell proliferation. Since the patient takes anti-inflammatory drugs in the first few days and these drugs interact pharmacologically with the growth factor, it can be concluded that the best concentration for the growth factor is nanofiber with a concentration of 0.612 ng/mg, which in the early days of the low release of the growth factor and do not delay lesion healing due to controlled release and have the best cell proliferation [40].

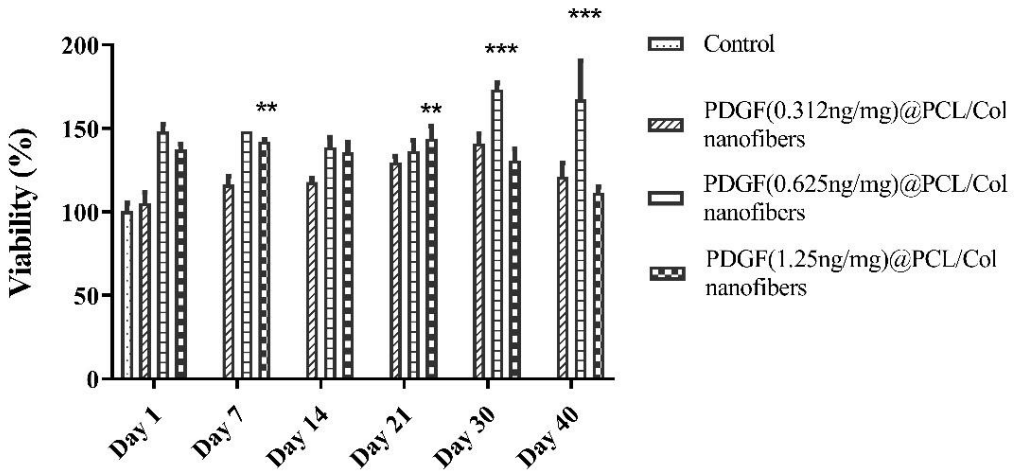

Figure 6. Cell proliferation results of PDGF nanofibers. A phosphate buffer was added as a control group. Data are represented as mean ± SD from three independent tests. (***$P < 0.05$ vs. control).

2.6. Effect of released PDGF on gene expression of osteogenic markers

The biological effect of released PDGF on expression levels of osteoblastic differentiation markers, RUNX2 and IBSP, and COX-2 in MG-63 cells were evaluated by semi-quantitative RT-PCR [41] at different intervals. The osteogenesis ability of nanofibers was evaluated to investigate the PDFG bioactivity and function maintenance after release. As shown in Figure 7, PDGF (0.625 ng/mg) @PCL/Col and PCL/Col (control group) were used at the first hours (h1), third hours (h3), first day (d1) and seventh days (d2) of culture. The expression of Runx2 was significantly higher after 24 hours compared to the first and third hours in the scaffolds and then this level was dramatically lower on the 7th day. Runx2 plays a vital role as a transcription factor responsible for regulating osteoblast differentiation which reaches its expression peak in immature osteoblasts and is subsequently reduced in mature osteoblasts [42]. PDGF (0.625 ng/mg) @PCL/Col fibers significantly enhanced the expression and maturation of RUNX-2 during the initial stages. Laflamme *et al*. [43] showed that epidermal growth factor alone or in combination with bone morphogenetic proteins plays an active role in osteoblast proliferation and protein (osteocalcin, Runx2, and ALP) expression. Currently, the FDA has approved products such as OP-1™ Implants and INFUSE™ collagen sponge bone grafts, utilizing BMP7 and BMP2, respectively [44, 45]. Additionally, rhPDGF-BB has received approval under the trade name AUGMENT® Bone Graft for clinical orthopedic applications [46].

As evidenced by the real-time PCR results, the released PDGF was biologically active and was able to induce the expression of two osteogenic factors RUNX-2 and IBSP. The expression was significantly increased during the first day of PDGF release. However, in both cases, the expression levels were back to normal after the week. The level of upregulation was much higher in IBSP. Results from real-time PCR also indicated an increase in COX-2 expression compared to the control group in the very first hours of release. The pattern of upregulation was in agreement with the results of the release test in which a burst in the release of PDGF was obvious on the first day.

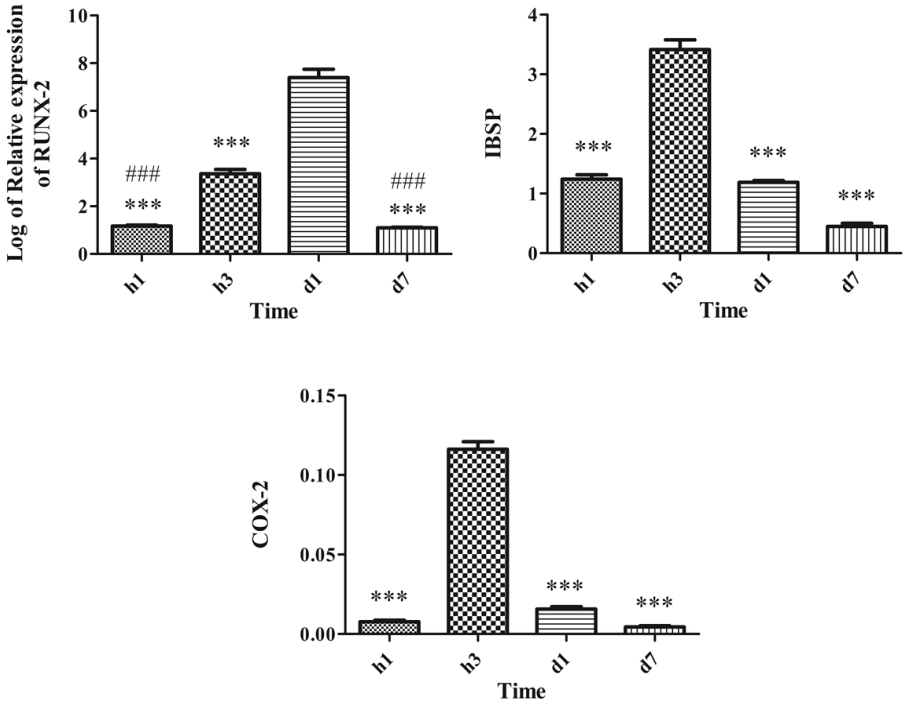

Figure 7. The osteogenic-related gene expression of core-shell nanofibers in osteogenic induction at different intervals. Data values are presented as mean ± SD from three repeated tests. (***P < 0.05 vs. d1, ###P < 0.05 vs. h3 for RUNX-2 and ***P < 0.05 vs. h3 for IBSP and COX-2).

3. CONCLUSION

In this study, we developed a novel core/shell fiber through electrospinning for use as a GTR membrane, enabling sustained-release of PDGF. Loading PDGF significantly changed the fiber morphology, with SEM images revealing PDGF entrapment in the swollen parts of the fibers. Incorporating PDGF enhanced the cytocompatibility of the PCL/Col membrane, and the PDGF@PCL/Col fibers exhibited impressive bone cell proliferation. The enhanced expression of osteogenic genes indicates the fibers' potential to support osteogenesis after PDGF integration. The obtained results point out that the membrane design in this study presents a new and effective method for delivering growth factors into periodontal tissue.

4. MATERIALS AND METHODS

4.1. Materials

Polycaprolactone (PCL, Mw = 80 kDa), and collagen from bovine Achilles' tendon all were achieved by Sigma-Aldrich company of USA. Dichloromethane, MTT (3- (4 and 5-dimethyl thiazole-2-il) -2 and 5 d-phenyltetrahydramide), and Ethanol were bought from Merck. Human PDGF-BB platinum ELISA kit (BMS2071, Invitrogen), Recombinant Human PDGF‑BB solutions: (220-BB, R&D systems), Streptomycin-Penicillin, FBS, and DMEM culture medium from Gibco of Germany were used.

4.2. Methods

4.2.1. Electrospinning

PCL and Col solutions were prepared separately at 9 and 70 %w/w concentrations. PCL was dissolved in a mixture of dichloromethane and ethanol (60:40) at room temperature for 30 minutes to achieve the 9 wt. % concentration. The preparation of Col solution (70% w/w) in water was performed at room temperature using a laboratory magnetic stirrer for 24 h. To investigate the electrospinning ability of the prepared solutions, the applied voltage parameters (8, 12, 16, 20 kV), the feed rate of the core-shell solutions (1:1, 1:3, 1:5), flow rate (0.25 ml/h), and tip-to-collector distance (12 cm) were used. By changing the above

parameters here PCL/Col fibers were prepared as core-shell. Co-axial nozzles of 14 gauges for shell solution and 18 gauges for core solution were used.

4.2.2. PDGF Loading

After identifying the optimal fibers, the GF-loaded solutions were prepared by adding 50, 100, and 200 µl of GF solutions with a concentration of 0.25ng/ml to the core polymer blend solution (equal to 0.312ng/mg, 0.625ng/mg, and 1.25ng/mg of the polymer(s) weight). This solution was homogenized by pipetting to ensure the complete dissolution of the GF [33].

4.2.3. Characterization

The morphology of membranes were evaluated using scanning electron microscopy (SEM; FEI Model Quanta 450 FEG, Hillsboro, OR, USA) and field-effect scanning electron microscopy (FE-SEM) -(TSCAN - Czech nation) at an accelerating voltage of 5-30 kV. Before observation, the membranes were mounted on metal stubs by using conductive double-sided tapes and subsequently sputter-coated with gold. The morphology and the diameters of fiber samples were also observed by transmission electron microscopy (TEM, JEOL 2100F). Then, the fiber's diameters were measured by the Digimizer software at 100 random locations for each membrane. The fibers were characterized by using Fourier transform infrared spectroscopy (FT-IR) -(Shimadzu IR-prestige 21). To measure the FT-IR spectrum of the fiber's membrane, 2 mg of the samples were mixed with 10 mg KBr and compressed into a tablet form. The IR spectra of these tablets were obtained in a transition mode and the spectral region of 400 to 4000 cm^{-1}.

4.2.4. In vitro PDGF release and kinetics study

5 mg of fiber mats loaded with the desired amount of growth factor (0.312ng/mg, 0.625ng/mg, and 1.25ng/mg fibers) were immersed in an amicon tube containing a 10 ml phosphate buffer 0.2 M with pH 7.4. After different time intervals, 0.5 ml of the release buffer was replaced with fresh buffer and kept in the refrigerator. The drug release concentrations were evaluated by the ELISA method at λmax 260 nm. ELISA was performed using the Human PDGF-BB platinum ELISA kit (BMS2071, Invitrogen) kit according to the manufacturer's instructions. Briefly, after preparing reagents, working standards, and samples 50 µl of sample or standard was added to appropriate wells. Then 50 µl of the Antibody Cocktail was added to each well. Plates were sealed and incubated for 1 hour at room temperature on a plate shaker set to 400 rpm. In the next step, wells were washed 3 times using 350 µl 1X Wash Buffer followed by decanting after at least 10 seconds. After the last wash excess liquid was removed and 100 µl of TMB development solution was added to each well and incubated for 10 minutes in the dark while shaking for 20 minutes. 100 µl of stop solution was added to each well and the OD at 450 nm was recorded.

All release experiments were carried out in triplicate. The cumulative release of the growth factor was determined by the following equation:

$$\text{Cumulative release } (\%) = \frac{\sum_{i-1}^{n-1} C_i + 25 \times C_n}{\text{amount of total drug}} \times 100$$

where C_n and C_i represent the growth factor concentration measured by UV spectrophotometer at the time of n and i, respectively.

For *in vitro* release kinetics evaluation, several approaches can be used such as analysis of variance, model-independent, and model-dependent approaches. In this study, model-dependent approaches were used for the comparison of dissolution profiles. In model-dependent approaches, release data were fitted to kinetic models including the zero-order (Eq. 1), first-order (Eq. 2), and Higuchi matrix (Eq. 3) release equations to find the equation with the best fit.

$$C = k_0 t \quad (1)$$

$$\text{Log } C = \text{Log } C_0 - kt/2.303 \quad (2)$$

$$Q = kt^{1/2} \quad (3)$$

In (Eq.1) and (Eq. 2), C0 is the initial concentration of the drug, k is the first-order rate constant, and t is the time. In (Eq.3), Q is the amount of drug released in time (t) per unit area and k is the Higuchi dissolution constant [47].

4.2.5. Cell culture and cell viability assessment

MG-63 cell was obtained from the National Cell Bank of Iran (NCBI, Pasteur Institute of Iran, Tehran, Iran). Cells were cultured in high glucose DMEM (BI-1003Idezist Notarkib, Iran) supplemented with 10% FBS (BI-1201, Idezist Notarkib, Iran) and PEN-STREP solution (BI-1203, Idezist Notarkib, Iran). Cells were maintained at 37°C in a humidified incubator supplemented with 5% CO_2. The flask media were changed every three days.

Cytotoxicity of fiber was evaluated by 4,5-dimethylthiazol-2-yl)-2,5-diphenyl tetrasodium bromide (MTT) assay (M2003-1G, Sigma- Aldrich). 100 µl cell suspension (1×10^6/ml) in high glucose DMEM supplemented with 10% FBS was seeded in 96-well plates and incubated overnight to reach 90-100% confluency. On the following day, 300 µl of Sterilized samples of fiber were added to each well, and cells were incubated for 24 h. According to Füsun Acartürk *et al*, [48] to obtain sterilized samples of fibers, fibers were irradiated with a UV lamp (254 nm) in a UV box cabinet (Sahandazar, Tabriz, Iran) for 3 h followed by immersion in sterile DMEM at 37℃ for 24 h. After incubation, fibers were removed from DMEM and the supernatant was used. On the next day, the medium was aspirated and 200 µl of fresh DMEM and 20 µl of MTT-containing medium (1 mg/ml) were added into each well. After incubation for 4 hours, the medium was aspirated and dimethyl sulfoxide (200 µl/well) was added to stop the reaction. The optical density was quantified in a multi-detection microplate reader, Synergy™ HT (BioTek Instruments Inc.) at 570 nm wavelength. The percentage of cell viability was calculated by comparing the optical density of each well to control (no treatment) cells [31].

4.2.6. Cell proliferation assay

MG-63 cells (5 x 10^3 cells/wells) were seeded into a 48-well cell culture plate. The 20 µl released MG-63 cells (5 x 10^3 cells/wells) were seeded into a 48-well cell culture plate. The 20 µl released samples were added to the wells. After overnight incubation, the culture medium was replaced with 200 ml of 1% glutaraldehyde and incubated at 37°C in a humidified air 5% CO_2 incubator for 15 minutes. The wells were washed with 300 µl of 1X sterile PBS with pH 7.4, and 200 ml of 0.02% crystal violet was added to the wells and incubated for 30 minutes. The wells were rinsed with sterile distilled water for 15 minutes to remove dead cells from the environment due to lack of adhesion, and only living cells were used during the test to check for light absorption. The cells were exposed to 360 microliters of 70% ethanol for 3 hours. Sample absorption at a wavelength of 578 nm was read by the plate reader device [49].

4.2.7. RT-PCR

To evaluate the ability of the released PDGF to induce the expression of osteoblastic differentiation markers to induce cell COX-2 pathway, relative expression of runt-related transcription factor 2 (RNUX-2), Homo sapiens integrin-binding sialoprotein (IBSP), and cyclooxygenase-2 (COX-2) were evaluated. PDGF (0.625 ng/mg)@PCL/Col fibers (based on containing 100 ng PDGF) and PCL/Col fiber were weighed. Collected Release samples from 1 hour, 3 hours, 1 day, and 7 days after the start of the release test were used to evaluate the relative expression of the abovementioned genes. One million cells of MG-63 were cultured in cell culture plates for 6 hours. After the cells reached 90% density, the supernatant culture medium was discarded and the complete culture medium containing 5% bovine fetal serum and 100 µl of each release sample was added to each well. The cells were stored in a 37 °C incubator for 5 hours with 5% CO_2 and after 24 hours the total RNA was extracted using the CinnaPure RNA (CinnaGen, Iran) according to the manufacturer's instructions. The quality and concentration of extracted RNA were evaluated by spectrophotometer (NanoDrop 2000, USA). Total RNA was then used to prepare cDNA. cDNA synthesis was performed using the cDNA Synthesis Kit (YT4500, YTA, Iran) according to the manufacturer's instructions. The relative expression of RNUx-2 and IBSP genes was determined using specific primers (Table 2) and Super SYBR Green qPCR mastermix (YT2552, YTA, Iran) [41]. The GAPDH gene was used as an internal control. All experiments were repeated at least twice.

Table 2. List of primers used for Real-time Quantitative PCR Analysis.

Num	Gene Name		Primer Sequence
1	RUNX-2	Forward Primer sequence	CGAAATGCCTCCGCTGTTAT
		Reverse primer sequence	CGCTCCGGCCCACAA
2	IBSP	Forward Primer sequence	GCGAAGCAGAAGTGGATGAAA
		Reverse primer sequence	TGCCTCTGTGCTGTTGGTACTG
3	COX-2	Forward Primer sequence	TGCATTCTTTGCCCAGCACT
		Reverse primer sequence	AAAGGCGCAGTTTACGCTGT

Relative quantification PCR was performed by LightCycler® 96 System using the following thermal cycling conditions summarized in Table 3. Relative quantification was performed according to the Pfaffl method (Eq. 4) and (Eq. 5).

$$\text{mRNA expression ratio} = 2^{-\Delta\Delta CT} \quad \text{(Eq. 4)}$$

$$\Delta\Delta CT = \Delta CT \text{ sample} - \Delta CT \text{ control} \quad \text{(Eq. 5)}$$

In each calculation, sample refers to cells that were treated with fiber, PDGF containing fiber or PDGF and control refers to equivalent no treatment groups.

Table 3. Thermal cycling conditions for relative quantification PCR performed by LightCycler® 96 System.

Initial Denaturation	94 °C	3 min	Hold
Denature	95 °C	10 sec	40 Cycles
Anneal	Tm-5 °C	10 sec	
Extend	72 °C	20 sec	
Melting curve analysis			

4.2.8. Statistical Analyses

All quantitative results were obtained from triplicate samples. Every data point was expressed as mean ± SD. One-way analysis of variance using Tukey's test was performed to compare the results. The statistical significance of variations could be confirmed at $P < 0.05$.

Acknowledgments: The authors gratefully acknowledge the research council of Kermanshah University of Medical Sciences [Grant Number. 97712] for financial support.

Author contributions: Concept – L.B., M.R.; Design – L.B., M.R.; Supervision – L.B.; Resources –L.B.; Materials – L.B.; Data Collection and/or Processing – M.L., P.M.; Analysis and/or Interpretation – M.L., P.M.; Literature Search – M.L., P.M., Z.P.; Writing – Z.P.; Critical Reviews – L.B., M.R.

Conflict of interest statement: The authors declare that they have no known competing financial interests or personal relationships that could have appeared to influence the work reported in this paper.

REFERENCES

[1] Scannapieco FA, Gershovich E. The prevention of periodontal disease—An overview. Periodontol 2000. 2020;84(1):9-13. https://doi.org/10.1111/prd.12330

[2] Mirzaeei S, Ezzati A, Mehrandish S, Asare-Addo K, Nokhodchi A. An overview of guided tissue regeneration (GTR) systems designed and developed as drug carriers for management of periodontitis. J Drug Deliv Sci Technol. 2022;71:103341-103352. https://doi.org/10.1016/j.jddst.2022.103341

[3] Woo HN, Cho YJ, Tarafder S, Lee CH. The recent advances in scaffolds for integrated periodontal regeneration. Bioact Mater. 2021 Mar 18;6(10):3328-3342. https://doi.org/10.1016/j.bioactmat.2021.03.012

[4] Gao Y, Wang S, Shi B, Wang Y, Chen Y, Wang X, Lee ES, Jiang HB. Advances in modification methods based on biodegradable membranes in guided bone/tissue regeneration: A review. Polymers. 2022;14(5):871-894. https://doi.org/10.3390/polym14050871
[5] Liang Y, Luan X, Liu X. Recent advances in periodontal regeneration: A biomaterial perspective. Bioact Mater. 2020;5(2):297-308. https://doi.org/10.1016/j.bioactmat.2020.02.012
[6] Song E, Yeon Kim S, Chun T, Byun HJ, Lee YM. Collagen scaffolds derived from a marine source and their biocompatibility. Biomaterials. 2006 May;27(15):2951-2961. https://doi.org/10.1016/j.biomaterials.2006.01.015
[7] Pina S, Oliveira JM, Reis RL. Natural-based nanocomposites for bone tissue engineering and regenerative medicine: A review. Adv Mater. 2015;27(7):1143-1169. https://doi.org/10.1002/adma.201403354
[8] Guo S, He L, Yang R, Chen B, Xie X, Jiang B, Weidong T, Ding Y. Enhanced effects of electrospun collagen-chitosan nanofiber membranes on guided bone regeneration. J Biomater Sci Polym Ed. 2020;31(2):155-168. https://doi.org/10.1080/09205063.2019.1680927
[9] Xie Y, Zinkle A, Chen L, Mohammadi M. Fibroblast growth factor signalling in osteoarthritis and cartilage repair. Nat Rev Rheumatol. 2020;16(10):547-564. https://doi.org/10.1038/s41584-020-0469-2
[10] Ren X, Zhao M, Lash B, Martino MM, Julier Z. Growth factor engineering strategies for regenerative medicine applications. Front Bioeng Biotechnol. 2020;7:469-478. https://doi.org/10.3389/fbioe.2019.00469
[11] Yamakawa S, Hayashida K. Advances in surgical applications of growth factors for wound healing. Burns Trauma. 2019;7:10. https://doi.org/10.1186/s41038-019-0148-1
[12] Zarei F, Soleimaninejad M. Role of growth factors and biomaterials in wound healing. Artif Cells Nanomed Biotechnol. 2018;46(sup1):906-911. https://doi.org/10.1080/21691401.2018.1439836
[13] Janssens K, ten Dijke P, Janssens S, Van Hul W. Transforming growth factor-beta1 to the bone. Endocr Rev. 2005;26(6):743-774. https://doi.org/10.1210/er.2004-0001
[14] Ambekar RS, Kandasubramanian B. Advancements in nanofibers for wound dressing: A review. Eur Polym J. 2019;117:304-336. https://doi.org/10.1016/j.eurpolymj.2019.05.020
[15] Chen K, Hu H, Zeng Y, Pan H, Wang S, Zhang Y, Shi L, Tan G, Pan W, Liu H. Recent advances in electrospun nanofibers for wound dressing. Eur Polym J. 2022; 178:111490. https://doi.org/10.1016/j.eurpolymj.2022.111490
[16] Pant B, Park M, Park S-J. Drug delivery applications of core-sheath nanofibers prepared by coaxial electrospinning: A review. Pharmaceutics. 2019;11(7):305. https://doi.org/10.3390/pharmaceutics11070305
[17] Dwivedi P, Han S, Mangrio F, Fan R, Dwivedi M, Zhu Z, Huang F, Wu Q, Khatik R, Cohn DE, Si T, Hu S, Sparreboom A, Xu RX. Engineered multifunctional biodegradable hybrid microparticles for paclitaxel delivery in cancer therapy. Mater Sci Eng C. 2019;102:113-123. https://doi.org/10.1016/j.msec.2019.03.009
[18] Qin X. Coaxial electrospinning of nanofibers. Electrospun nanofibers: Elsevier; 2017. p. 41-71. https://doi.org/10.1016/B978-0-08-100907-9.00003-9
[19] Lu Y, Huang J, Yu G, Cardenas R, Wei S, Wujcik EK, Guo Z. Coaxial electrospun fibers: applications in drug delivery and tissue engineering. Wiley Interdiscip Rev Nanomed Nanobiotechnol. 2016;8(5):654-677. https://doi.org/10.1002/wnan.1391
[20] Rafiei M, Jooybar E, Abdekhodaie MJ, Alvi M. Construction of 3D fibrous PCL scaffolds by coaxial electrospinning for protein delivery. Mater Sci Eng C. 2020;113:110913. https://doi.org/10.1016/j.msec.2020.110913
[21] Wang N, Zhao Y. Coaxial electrospinning. Electrospinning: Nanofabrication and Applications: Elsevier; 2019. p. 125-200. https://doi.org/10.1016/B978-0-323-51270-1.00005-4
[22] Pihlstrom BL, Michalowicz BS, Johnson NW. Periodontal diseases. Lancet. 2005;366(9499):1809-1820. https://doi.org/10.1016/S0140-6736(05)67728-8
[23] Mizraji G, Davidzohn A, Gursoy M, Gursoy UK, Shapira L, Wilensky A. Membrane barriers for guided bone regeneration: An overview of available biomaterials. Periodontol 2000. 2023;93(1):56-76. https://doi.org/10.1111/prd.12502
[24] Liu X, He X, Jin D, Wu S, Wang H, Yin M, Aldalbahi A, El-Newehy M, Mo X, Wu J. A biodegradable multifunctional nanofibrous membrane for periodontal tissue regeneration. Acta Biomater. 2020;108:207-222. https://doi.org/10.1016/j.actbio.2020.03.044
[25] Kim K, Su Y, Kucine AJ, Cheng K, Zhu D. Guided bone regeneration using barrier membrane in dental applications. ACS Biomater Sci Eng. 2023;9(10):5457-5478. https://doi.org/10.1021/acsbiomaterials.3c00690
[26] Cheng G, Yin C, Tu H, Jiang S, Wang Q, Zhou X, Xing X, Xie C, Shi X, Du Y, Deng H, Li Z. Controlled co-delivery of growth factors through layer-by-layer assembly of core–shell nanofibers for improving bone regeneration. ACS Nano. 2019;13(6):6372-6382. https://doi.org/10.1021/acsnano.8b06032
[27] Dems D, Rodrigues da Silva J, Hélary C, Wien F, Marchand M, Debons N, Muller L, Chen Y, Schanne-Klein MC, Laberty-Robert C, Krins N, Aimé **C**. Native collagen: electrospinning of pure, cross-linker-free, self-supported membrane. ACS Appl Bio Mater. 2020;3(5):2948-2957. https://doi.org/10.1021/acsabm.0c00006
[28] Moradipour P, Limoee M, Janfaza S, Behbood L. Core-shell nanofibers based on polycaprolactone/polyvinyl alcohol and polycaprolactone/collagen for biomedical applications. J Pharm Innov. 2021;17:911-920. https://doi.org/10.1007/s12247-021-09568-z
[29] Lv Y-Y, Wu J, Wan L-S, Xu Z-K. Novel porphyrinated polyimide nanofibers by electrospinning. J Phys Chem C 2008;112(29):10609-10615. https://doi.org/10.1021/jp7105549

[30] Cianciolo G, Stefoni S, Zanchelli F, Iannelli S, Colì L, Borgnino LC, De Sanctis LB, Stefoni V, De Pascalis A, Isola E, La Hanna G. PDGF-AB release during and after haemodialysis procedure. Nephrol Dial Transplant. 1999;14(10):2413-2419. https://doi.org/10.1093/ndt/14.10.2413
[31] Yamano S, Ty L, Dai J. Bioactive collagen membrane as a carrier for sustained release of PDGF. J Tissue Sci Eng. 2011;02(04). https://doi.org/10.4172/2157-7552.1000110
[32] Gerstenfeld LC, Cullinane DM, Barnes GL, Graves DT, Einhorn TA. Fracture healing as a post-natal developmental process: molecular, spatial, and temporal aspects of its regulation. J Cell Biochem. 2003;88(5):873-884. https://doi.org/10.1002/jcb.10435
[33] Liao IC, Chew SY, Leong KW. Aligned core-shell nanofibers delivering bioactive proteins. Nanomedicine (London, England). 2006;1(4):465-471. https://doi.org/10.2217/17435889.1.4.465
[34] Kagami S, Kondo S, Löster K, Reutter W, Kuhara T, Yasutomo K, Kuroda Y. α1β1 integrin-mediated collagen matrix remodeling by rat mesangial cells is differentially regulated by transforming growth factor-β and platelet-derived growth factor-BB. J Am Soc Nephrol. 1999;10(4):779-789. https://journals.lww.com/jasn/toc/1999/04000
[35] Khatami N, Khoshfetrat AB, Khaksar M, Zamani ARN, Rahbarghazi R. Collagen-alginate-nano-silica microspheres improved the osteogenic potential of human osteoblast-like MG-63 cells. J Cell Biochem. 2019;120(9):15069-15082. https://doi.org/10.1002/jcb.28768
[36] Kim HK, Kim M-G, Leem K-H. Collagen hydrolysates increased osteogenic gene expressions via a MAPK signaling pathway in MG-63 human osteoblasts. Food Funct. 2014;5(3):573-578. https://doi.org/10.1039/C3FO60509D
[37] Sahoo S, Ang LT, Goh JCH, Toh SL. Growth factor delivery through electrospun nanofibers in scaffolds for tissue engineering applications. J Biomed Mater Res A. 2010;93(4):1539-1550. https://doi.org/10.1002/jbm.a.32645
[38] Behring J, Junker R, Walboomers XF, Chessnut B, Jansen JA. Toward guided tissue and bone regeneration: morphology, attachment, proliferation, and migration of cells cultured on collagen barrier membranes. A systematic review. Odontology. 2008;96(1):1-11. https://doi.org/10.1007/s10266-008-0087-y
[39] Strayhorn CL, Garrett JS, Dunn RL, Benedict JJ, Somerman MJ. Growth factors regulate expression of osteoblast-associated genes. J Periodontol. 1999;70(11):1345-1354. https://doi.org/10.1902/jop.1999.70.11.1345
[40] Limoee M, Moradipour P, Godarzi M, Arkan E, Behbood L. Fabrication and in-vitro investigation of polycaprolactone-(polyvinyl alcohol/collagen) hybrid nanofiber as anti-inflammatory guided tissue regeneration membrane. Curr Pharm Biotechnol. 2019;20(13):1122-1133. https://doi.org/10.2174/1389201020666190722161004
[41] Pfaffl MW. A new mathematical model for relative quantification in real-time RT-PCR. Nucleic Acids Res. 2001;29(9):e45. https://doi.org/10.1093/nar/29.9.e45
[42] Komori T. Regulation of proliferation, differentiation and functions of osteoblasts by Runx2. Int J Mol Sci. 2019;20(7):1694-1705. https://doi.org/10.3390/ijms20071694
[43] Laflamme C, Curt S, Rouabhia M. Epidermal growth factor and bone morphogenetic proteins upregulate osteoblast proliferation and osteoblastic markers and inhibit bone nodule formation. Arch Oral Biol. 2010;55(9):689-701. https://doi.org/10.1016/j.archoralbio.2010.06.010
[44] McKay WF, Peckham SM, Badura JM. A comprehensive clinical review of recombinant human bone morphogenetic protein-2 (INFUSE® Bone Graft). Int Orthop. 2007;31:729-734. https://doi.org/10.1007/s00264-007-0418-6
[45] White AP, Vaccaro AR, Hall JA, Whang PG, Friel BC, McKee MD. Clinical applications of BMP-7/OP-1 in fractures, nonunions and spinal fusion. Int Orthop. 2007;31:735-741. https://doi.org/10.1007/s00264-007-0422-x
[46] Daniels TR, Anderson J, Swords MP, Maislin G, Donahue R, Pinsker E, Quiton JD. Recombinant Human Platelet–Derived Growth Factor BB in Combination with a Beta-Tricalcium Phosphate (RhPDGF-BB/β-TCP)-Collagen Matrix as an Alternative to Autograft. Foot Ankle Int. 2019;40(9):1068-1078. https://doi.org/10.1177/1071100719851468
[47] Rostami E, Kashanian S, Azandaryani AH. Preparation of solid lipid nanoparticles as drug carriers for levothyroxine sodium with in vitro drug delivery kinetic characterization. Mol Biol Rep. 2014;41(5):3521-3527. https://doi.org/10.1007/s11033-014-3216-4
[48] Tort S, Demiröz FT, Yıldız S, Acartürk F. Effects of UV exposure time on nanofiber wound dressing properties during sterilization. J Pharm Innov. 2020;15:325-332. https://doi.org/10.1007/s12247-019-09383-7
[49] Dai J, Jian J, Bosland M, Frenkel K, Bernhardt G, Huang X. Roles of hormone replacement therapy and iron in proliferation of breast epithelial cells with different estrogen and progesterone receptor status. Breast (Edinburgh, Scotland). 2008;17(2):172-179. https://doi.org/10.1016/j.breast.2007.08.009